

High speed self-testing quantum random number generation without detection loophole

Yang Liu,^{1,2} Xiao Yuan,^{1,2,3} Ming-Han Li,^{1,2} Weijun Zhang,⁴ Qi Zhao,³ Jiaqiang Zhong,⁵ Yuan Cao,^{1,2} Yu-Huai Li,^{1,2} Luo-Kan Chen,^{1,2} Hao Li,⁴ Tianyi Peng,³ Yu-Ao Chen,^{1,2} Cheng-Zhi Peng,^{1,2} Sheng-Cai Shi,⁵ Zhen Wang,⁴ Lixing You,⁴ Xiongfeng Ma,³ Jingyun Fan,^{1,2} Qiang Zhang,^{1,2} and Jian-Wei Pan^{1,2}

¹*Shanghai Branch, National Laboratory for Physical Sciences at Microscale and Department of Modern Physics, University of Science and Technology of China, Shanghai 201315, P. R. China*

²*Shanghai Branch, CAS Center for Excellence and Synergetic Innovation Center in Quantum Information and Quantum Physics, University of Science and Technology of China, Shanghai 201315, P. R. China*

³*Center for Quantum Information, Institute for Interdisciplinary Information Sciences, Tsinghua University, Beijing 100084, P. R. China*

⁴*State Key Laboratory of Functional Materials for Informatics, Shanghai Institute of Microsystem and Information Technology, Chinese Academy of Sciences, Shanghai 200050, P. R. China*

⁵*Purple Mountain Observatory and Key Laboratory of Radio Astronomy, Chinese Academy of Sciences, 2 West Beijing Road, Nanjing, Jiangsu 210008, P. R. China*

Abstract

Quantum mechanics provides means of generating genuine randomness that is impossible with deterministic classical processes. Remarkably, the unpredictability of randomness can be certified in a self-testing manner that is independent of implementation devices. Here, we present an experimental demonstration of self-testing quantum random number generation based on an detection-loophole free Bell test with entangled photons. In the randomness analysis, without the assumption of independent identical distribution, we consider the worst case scenario that the adversary launches the most powerful attacks against quantum adversary. After considering statistical fluctuations and applying an $80 \text{ Gb} \times 45.6 \text{ Mb}$ Toeplitz matrix hashing, we achieve a final random bit rate of 114 bits/s , with a failure probability less than 10^{-5} . Such self-testing random number generators mark a critical step towards realistic applications in cryptography and fundamental physics tests.

Introduction.— Random numbers are widely used in applications ranging from numerical simulation and cryptography to lottery. While the foremost property of random number generators (RNGs) in many applications is distribution uniformity of its outputs, secure information processing applications such as cryptography demand additionally that the devices to produce randomness must be secure against any adversaries, regardless of classical or quantum mechanics. Classical RNGs have a deterministic nature and hence are not random. Quantum random number generators (QRNGs) rely on the unpredictability in breaking quantum coherence and are theoretically unpredictable. However, the unpredictability may be jeopardized in practice because the adversary may gain information about the devices and even maliciously manipulate the devices of QRNGs, which is often undetected by a finite set of statistical tests. Self-testing QRNGs certify the randomness unconditionally based on the loophole free violation of Bell’s inequality, offering a reliable way of generating genuine randomness in a device-independent manner and therefore holding great promise for future applications. (See Ref. [1, 2] for a review of QRNGs.)

Considering a loophole free Bell test experiment. Alice and Bob are honest parties at two remote sites, each receives one of a pair of entangled photons and measures its quantum state with a randomly selected measurement setting. Alice and Bob may not trust the devices because the devices may be prepared by the adversary. The experiment observes no-signaling theorem, *i.e.*, even at the speed of light, no information of measurement setting is conveyed to the source prior to the emission of entangled photon pairs (to close randomness loophole) and no information about Alice’s (Bob’s) measurement setting and measurement outcomes are conveyed to Bob (Alice) prior to his (her) state measurement (to close locality loophole). The photon-detection efficiency is sufficiently high for the experiment to be free from the detection loophole. Local hidden variable theories (based on classical determinism) set a bound to the correlation measurement between Alice and Bob. Breaking the bound exhibits quantum correlation, which cannot be explained by classical deterministic mechanisms. This nonlocal quantum correlation certifies that Alice and Bob’s measurement outcomes possess genuine quantum randomness which is inaccessible to the adversary, irrelevant to the implementation devices [3, 4].

As we deepen the understanding of self-testing QRNG [5–13], the security analysis becomes more efficient in producing randomness and more robust to noise. In particular, the entropy accumulation theorem formulated by Dupuis, Fawzi, and Renner [12] converts

a single-shot result to the multiple-shot case. Exploiting the entropy accumulation theorem, Arnon-Friedman, Renner and Vidick proposed a self-testing QRNG analysis method without the assumption of independent identical distribution (i.i.d.), which nevertheless produces randomness with yield approaching the value for the i.i.d. case [13]. The analysis is also against quantum adversary. So far there were two reported experimental studies on self-testing QRNG. One was based on a detection loophole free Bell test experiment with entangled ions [14], which produced random bits at a rate of 1.5×10^{-5} bit s^{-1} without the assumption of i.i.d. The analysis is against classical adversary. The other one was based on a detection loophole free Bell test experiment with entangled photons [15], which produced random bits at a rate of 0.4 bit s^{-1} , albeit with the assumption of i.i.d.

Very recently, several experiments demonstrated the violation of Bell's inequality with both locality and detection loopholes closed simultaneously [16–19]. It was also shown that the randomness loophole can be progressively addressed with cosmic RNGs [20–22], which take advantage of randomness at the remote celestial object to set the time constraint of local hidden variable mechanisms deep into the cosmic history. These works pave the way to construct a practical self-testing QRNG. Here we report an experimental realization of a self-testing QRNG based on a detection loophole free Bell test with entangled photon pairs, with randomness extraction of 114 bits s^{-1} and uniformity within 10^{-5} , which is a significant improvement over the previous experiment [14]. The randomness generation analysis is against the most powerful quantum adversary attacks and does not rely on the independent identical distribution assumption. Our experiment marks a critical step for generating self-testing QRNGs for practical applications.

Proposal.— The self-testing QRNG protocol is based on the Bell test experiment, namely a Clauser-Horne-Shimony-Holt game [23]. In each experimental trial, Alice and Bob perform state measurements upon receiving random inputs x and y and produce outputs a and b , respectively. According to local hidden variable models, the correlations described by probability distributions $p(ab|xy)$ in the i.i.d. scenario are factorable with $p(ab|xy) = \sum_{\lambda} p(\lambda)p(a|x, \lambda)p(b|y, \lambda)$. The J -value of the CHSH game satisfies an inequality,

$$J = \frac{1}{4} \sum_{abxy} \beta_{abxy} p(ab|xy) - 3/4 \leq 0, \quad (1)$$

where the pay-off coefficient is given by

$$\beta_{abxy} = \begin{cases} 1, & \text{if } a \oplus b = x \cdot y \\ 0 & \text{if } a \oplus b \neq x \cdot y \end{cases}, \quad (2)$$

with \oplus standing for plus modulo 2. Quantum theory allows $J > 0$ as opposed to local hidden variable models.

In practice, all Bell test experiments have finite statistics. Instead of approximating probability distributions based on the i.i.d. assumption, we introduce the Bell value J_i in experimental trial i ,

$$J_i = \begin{cases} 1, & \text{if } a_i \oplus b_i = x_i \cdot y_i \\ 0, & \text{otherwise} \end{cases}. \quad (3)$$

The CHSH game value is an average of J_i for all n experimental trials,

$$\bar{J} = \frac{1}{n} \sum_{j=1}^n J_j - 3/4. \quad (4)$$

Here, we consider the case that the average probability of measurement setting choice is unbiased, $p(xy) = 1/4$. Violating the inequality in Eq. (1), $\bar{J} > 0$, indicates the presence of genuine quantum randomness in the measurement outcomes. The randomness can be quantified by the smooth min-entropy $H_{\min}^{\varepsilon_s}(\mathbf{AB}|\mathbf{XY}E)$ based on the CHSH game value \bar{J} and the number of experiment trials [13], which is bounded by,

$$H_{\min}^{\varepsilon_s}(\mathbf{AB}|\mathbf{XY}E) \geq n \cdot R_{\text{opt}}(\varepsilon_s, \varepsilon_{\text{EA}}, \omega_{\text{exp}}). \quad (5)$$

Here \mathbf{A} (\mathbf{B}) and \mathbf{X} (\mathbf{Y}) denote the input and output sequences of Alice (Bob), respectively; E denotes side information of a general quantum adversary; ε_s is the smoothing parameter; ω_{exp} is the expected CHSH game value. ε_{EA} is the probability of aborting the protocol; $H_{\min}^{\varepsilon_s}(\mathbf{AB}|\mathbf{XY}E)$ describes the amount of unpredictable randomness that can be extracted from the outputs \mathbf{AB} against the inputs \mathbf{XY} and any adversary E ; as a conservative estimation, we take the lower bound $R_{\text{opt}}(\varepsilon_s, \varepsilon_{\text{EA}}, \omega_{\text{exp}})$ as the theoretical amount of randomness on average for each trial. $\varepsilon_{\text{QRNG}}^c$ is the *completeness* error, *i.e.*, the probability for a protocol to abort for an honest implementation is at most $\varepsilon_{\text{QRNG}}^c$. The lower bound for the smooth min-entropy $H_{\min}^{\varepsilon_s}(\mathbf{AB}|\mathbf{XY}E)$ is smaller when the average probability of measurement setting choice is biased (See Supplemental Materials).

We experimentally implement the self-testing QRNG with the following procedure,

1. Bell test:

- (a) In experimental trial i , Alice and Bob receive random inputs X_i and Y_i and produce outputs A_i and B_i , respectively.
- (b) We assign a CHSH game value J_i according to the pay-off in Eq. (3) and calculate the average pay-off according to Eq. (4).
- (c) We abort the protocol if $\bar{J} < \omega_{\text{exp}} - \delta_{\text{est}}$. Here the completeness error is upper bounded by $\varepsilon_{\text{QRNG}}^c \leq \exp(-2n\delta_{\text{est}}^2)$, where $\delta_{\text{est}} \in (0, 1)$ is the width of the statistical confidence interval for the Bell violation estimation test.

2. Randomness estimation: conditioned on the violation of Bell's inequality in the experiment, either the protocol aborts with probability greater than $1 - \varepsilon_{\text{EA}}$ or the experiment produces randomness given by Eq. (5).

3. Randomness extraction: for a given failure probability of less than 2^{-t_e} , we apply the Toeplitz-matrix hashing extractor with a matrix of size $n \times H_{\min}^{\varepsilon_s}(\mathbf{AB}|\mathbf{XYE}) - t_e$ to extract $H_{\min}^{\varepsilon_s}(\mathbf{AB}|\mathbf{XYE}) - t_e$ random bits that is ε_s close to the uniform distribution. Here, we set $t_e = 100$.

Experiment.— The experimental layout is shown in Fig. 1. We enclose a periodically poled potassium titanyl phosphate (PPKTP) crystal in a Sagnac loop. With the injection of pump pulses at wavelength of 780 nm and pulse width of 10 ns at a repetition rate of 100 kHz, the loop emits polarization-entangled photon pairs at the degenerate wavelength of 1560 nm via spontaneous parametric downconversion process. The two photons of the pair travel in opposite directions. They are subject to polarization state measurements by Alice and Bob and are detected by superconducting nanowire single-photon detectors (SNSPD). In each experimental trial, the dichotomic photon-detection results of SNSPDs, 1 for "click" and 0 for "no click", are time-tagged for correlation analysis.

In our experiment, the overall single photon detection efficiency is determined to be $78.6\% \pm 1.5\%$ for Alice and $80.2\% \pm 1.5\%$ for Bob [24]. The two-photon interference visibility is measured to be $99.5\% \pm 2\%$ ($97.8\% \pm 1.5\%$) in the horizontal (diagonal) basis. Using Eberhard's method [25], we generate nonmaximally entangled state, $\cos(20.5^\circ)|HV\rangle + \sin(20.5^\circ)|VH\rangle$ and set angles of half-wave plates in polarization state measurements to be

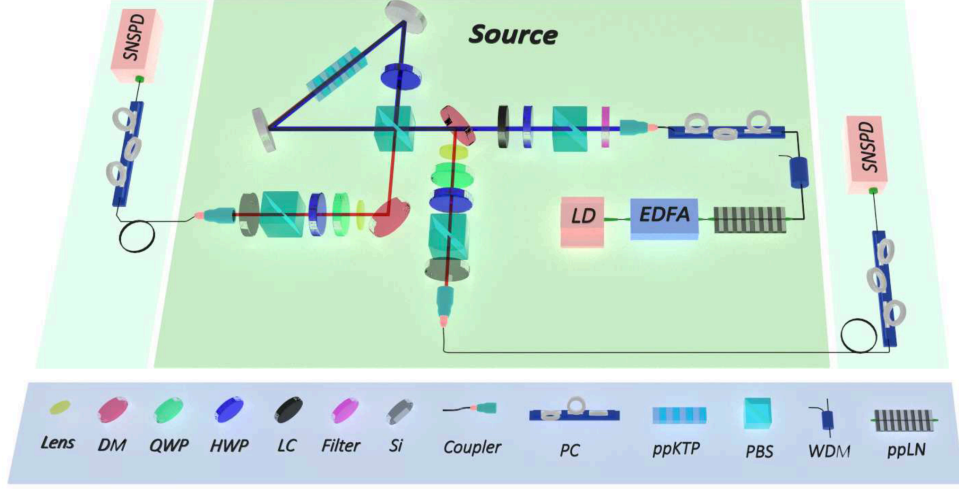


FIG. 1. Schematics for self-testing QRNG. Light pulses of 10 ns, 100 kHz from a 1560 nm seed laser (LD) are amplified by an erbium-doped fiber amplifier (EDFA), and up-converted to pulses at 780 nm via second-harmonic generation (SHG) in an in-line periodically poled lithium niobate (PPLN) waveguide. The residual 1560 nm light is removed by a wavelength-division multiplexer (WDM) and spectral filters. A half-wave plate (HWP) and a liquid crystal (LC) is used to adjust the pump polarization. The 780 nm light pulses are focused into a periodically poled potassium titanyl phosphate (PPKTP) crystal in a Sagnac loop to generate polarization entangled photon pairs. After removing the 780 nm pump pulses by dichroic mirrors (DMs) and a 1 mm thick silicon plate, the entangled photons at 1560 nm are subject to polarization state measurements and then sent to superconducting nanowire single-photon detectors (SNSPD) via 130 m optical fiber.

$A_1 = -84.0^\circ$ or $A_2 = -118.7^\circ$ for Alice, $B_1 = 6^\circ$ or $B_2 = -28.7^\circ$ for Bob, respectively, to have an optimum violation of Bell's inequality (see Supplemental Materials).

Previous Bell test experiments assigned measurement settings (xy) randomly with inputs from locally generated QRNGs [16–19]. RNGs including cosmic RNGs will be exploited to address the no-signaling issue in the input randomness [20–22]. For the current experiment, the settings are preset manually with parameters given by the Eberhard's optimization procedure as described above. The total photon detection efficiencies are high to close the detection loophole. We repeat the experiment by equal number of trials ($N = 1 \times 10^{10}$) per measurement setting choice xy and record the number of correlated events $N_{ab|xy}$ (see

Tab. I). According to Eq. (4-6), the J -value of the CHSH game is given by

$$J_N = J_{A_1B_1} + J_{A_1B_2} + J_{A_2B_1} + J_{A_2B_2} - 3/4, \quad (6)$$

with the Bell value J for settings $x = A_i$, $y = B_j$, and outputs ab given by

$$\begin{cases} J_{A_1B_1} = (N_{ab=00|A_1B_1} + N_{ab=11|A_1B_1})/N, \\ J_{A_1B_2} = (N_{ab=00|A_1B_2} + N_{ab=11|A_1B_2})/N, \\ J_{A_2B_1} = (N_{ab=00|A_2B_1} + N_{ab=11|A_2B_1})/N, \\ J_{A_2B_2} = (N_{ab=01|A_2B_2} + N_{ab=10|A_2B_2})/N. \end{cases} \quad (7)$$

For a total number of experimental trials $n = 4N = 4 \times 10^{10}$, the obtained J -value is 3.52×10^{-4} , indicating that our CHSH game rejects local hidden variable models. In our analysis, we set the expected CHSH game value to the one measured in the experiment, $\omega_{\text{exp}} = 3.52 \times 10^{-4}$, $\varepsilon_s = \varepsilon_{\text{EA}} = 1/\sqrt{n} = 5 \times 10^{-6}$ and $\delta_{\text{est}} = \sqrt{10/n} = 1.58 \times 10^{-5}$. Correspondingly, after applying an $80 \text{ Gb} \times 45.6 \text{ Mb}$ Toeplitz matrix hashing, the experiment produces 4.56×10^7 genuine random bits in total with uniformity within $\varepsilon_s + \varepsilon_{\text{EA}} = 10^{-5}$. The randomness generation speed is 0.00114 bits per trial or 114 bits/s, which is an improvement of $\times 10^7$ over the previous experiment [14]. With such a high yield, the stream of random bits pass the NIST statistic test suite for the first time of its kind (see Supplemental Materials).

TABLE I. Number of correlated events for equal number of trials (10^{10}) per measurement base settings: A_1B_1 , A_1B_2 , A_2B_1 and A_2B_2 . $a = 0$ or 1 indicates that Alice detects a photon or not, the same b for Bob. Mean photon number $\mu = 0.15$, violation $J_n = 3.52 \times 10^{-4}$.

Basis settings	$ab = 00$	$ab = 10$	$ab = 01$	$ab = 11$
A_1B_1	9780816728	49862593	57002217	112318462
A_1B_2	9574958251	41366122	263425568	120250059
A_2B_1	9577555854	253683380	46874032	121886734
A_2B_2	9255451323	361101111	365181363	18266203

With the same parameter setting, we plot the amount of randomness that can be produced by our experiment as a function of the number of experimental trials, which asymptotically approaches the optimal asymptotic value for i.i.d. as shown in Fig. 2. The amount of

randomness obtained in the current experiment is about 60% of the optimal asymptotic value.

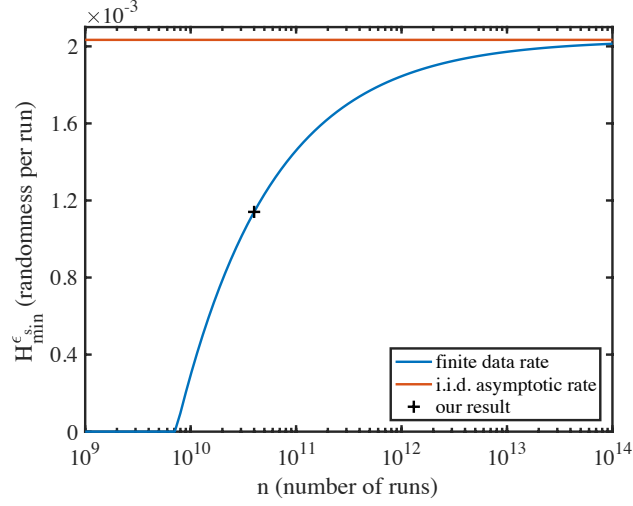


FIG. 2. Randomness generation versus number of experimental trials. We set the expected CHSH game value to be $\omega_{\text{exp}} = 3.52 \times 10^{-4}$, $\varepsilon_s = \varepsilon_{\text{EA}} = 1/\sqrt{n}$ and $\delta_{\text{est}} = \sqrt{10/n}$ for finite data rate.

One may expect to extract more randomness, even by orders of magnitude, for larger violations in the CHSH game with improved experimental parameters such as higher photon-detection efficiency, higher two-photon interference visibility, and optimized mean photon numbers (see Supplemental Materials), as shown in Fig. 4.

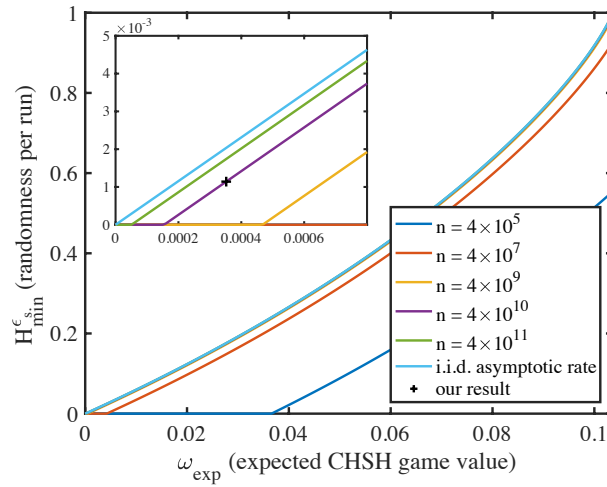


FIG. 3. Randomness generation versus expected CHSH game value. We set $\varepsilon_s = \varepsilon_{\text{EA}} = 1/\sqrt{n}$ and $\delta_{\text{est}} = \sqrt{10/n}$ for finite data rate curves.

Conclusion and outlook.— We implement a self-testing QRNG without the detection loophole, which does not need the assumption of identical and independent distribution and is against quantum adversary. We report randomness extraction at a rate of 114 bits/s with uniformity within 10^{-5} , marking a critical step in generating self-testing QRNG for secure information processing applications and tests of fundamental physics. One of the prospective works is to employ cosmic RNGs in a loophole free CHSH game such that the generated random bits are genuinely quantum-certified. Also, one can further speedup the randomness production by upgrading the utilized technology such as scaling up the operation repetition rate. One may note that the analysis method in Ref. [13] is efficient in producing quantum-certified randomness based on a CHSH game. However, it remains an open question what is the actual maximum extractable randomness in a CHSH game, furthermore, what is the maximum extractable randomness for a general nonlocal game.

Note added.— Recently, we become aware of a related work [26].

Acknowledgement.—The authors would like to thank Y. Shi for enlightening discussions. This work has been supported by the National Fundamental Research Program (under Grant No. 2013CB336800), the National Natural Science Foundation of China, the Chinese Academy of Science, and the 1000 Youth Fellowship program in China.

SUPPLEMENTAL MATERIAL

I. THEORY OF SELF-TESTING QUANTUM RANDOM NUMBER GENERATION

Here, we consider self-testing random number generation based on Bell test. Given a randomness source R as input, we can expand the input randomness by exploiting the protocol described below. At the end of the protocol, a classical string Z is returned. Conditioned on the random source R and a potential adversary's system E , the classical string Z is close to uniform. Note that E may be initially correlated to the implementation device. While running the protocol, the device is in the control of user and cannot signal to Eve. Before introducing the protocol, we define the soundness ε_{QRNG}^s and completeness ε_{QRNG}^c errors of a self-testing randomness generation protocol.

Definition 1. A randomness expansion protocol is $(\varepsilon_{QRNG}^c, \varepsilon_{QRNG}^s)$ -secure, if it satisfies:

1. *Soundness: For an untrusted device, it either aborts with probability less than P_{abort} or returns a string Z satisfying*

$$(1 - P_{\text{abort}}) \|\rho_{ZRE} - \rho_{U_m} \otimes \rho_{U_r} \otimes \rho_E\| \leq \varepsilon_{Q\text{RNG}}^s. \quad (8)$$

Here, ρ_{ZRE} denotes the state of the classical string Z , the input randomness source R and the system of Eve E ; ρ_{U_r} denotes a string of uniform random bits. The above inequality indicates that the output string is almost ($\varepsilon_{Q\text{RNG}}^s$) a uniform bit string and it has no correlation with the input randomness and the adversary Eve.

2. *Completeness: The honest device does not abort with probability greater than $1 - \varepsilon_{Q\text{RNG}}^c$.*

A. Protocol description

The inputs for the Bell test experiment are required to be random, which consumes random numbers. This inefficiency motivates the spot-checking protocol [11, 13, 27], where Bell test is only run with probability q (usually small) and the input is fixed with probability $(1 - q)$. A CHSH spot-checking protocol is shown as follows.

1. Bell test:

- (a) The game involves two players, Alice and Bob. Each player inputs a bit and is required to output a bit in each trial, for a total number of n trials. Denote their input and output bits in trial i to be X_i and Y_i and A_i and B_i , respectively.
- (b) Choose a bit string $\mathbf{t} = (t_1, \dots, t_n)$, for any $i \in \{1, 2, \dots, n\}$, $t_i \in \{0, 1\}$ according to the distribution $(1 - q, q)$.
- (c) If $t_i = 1$, this trial is a test trial, which is used to test the existence of adversary. Then Alice and Bob randomly input $X_i = \{0, 1\}$, $Y_i = \{0, 1\}$ and obtain $A_i = \{0, 1\}$, $B_i = \{0, 1\}$. In each trial, a score is recorded according to a pay-off function $J_i(A_i B_i X_i Y_i) \in \{0, 1\}$, which is given as follows.

$$J_i(A_i B_i X_i Y_i) = \begin{cases} 1 & A_i + B_i = X_i * Y_i \\ 0 & A_i + B_i \neq X_i * Y_i \end{cases} \quad (9)$$

- (d) If $t_i = 0$, this trial is a generation trial with fixed input string, $X_i = 0$, $Y_i = 0$ and $J_i = 0$.

(e) (c)-(d) steps are repeated in n trials.

(f) If $\sum_i J_i/n - 0.75 < \omega_{\text{exp}}q - \delta_{\text{est}}$, we abort the protocol. Otherwise, the protocol can be used for quantum random number generation. And the completeness error is upper bounded by $\varepsilon_{Q\text{RNG}}^c \leq \exp(-2n\delta_{\text{est}}^2)$.

2. Randomness estimation: conditioned on the Bell test is not aborted, either the protocol aborts with probability less than $\varepsilon_{Q\text{RNG}}^c$ or the amount of randomness is given by Eq. (10).
3. Randomness extraction: with failure probability less than 2^{-t_e} , we can extract $n \cdot R_{\text{opt}}(\varepsilon_s, \varepsilon_{EA}) - t_e$ random bits that is $\varepsilon_{Q\text{RNG}}^s$ close to a uniform distribution by using the Toeplitz-matrix hashing matrix.

B. Estimation of randomness production

In this work, we mainly focus on the security proof in Ref. [13]. The main tool of the security proof is based on the entropy accumulation theorem (EAT) [12], which can offer an avenue to reduce the complex multi-trial protocol to the i.i.d. case. After proving that the device independent protocol satisfies the requirements of an EAT channel, the entropy generated in the protocol can be analyzed based on the EAT theorem. Next, the randomness production based on the violation of CHSH inequality [28] under the stronger i.i.d. assumption can be connect to the non-i.i.d. case and gives a good lower bound for the generated randomness.

According to Theorem 10 of [13], the optimal randomness yield is given by

$$H_{\min}^{\varepsilon_s}(\mathbf{AB}|\mathbf{XY}E) \geq n \cdot R_{\text{opt}}(\varepsilon_s, \varepsilon_{EA}). \quad (10)$$

where the smoothed min-entropy $H_{\min}^{\varepsilon_s}(\mathbf{AB}|\mathbf{XY}E)$ evaluates the amount of extractable randomness, ε_s is the smoothing parameter, ε_{EA} is the error probability of the entropy accumulation protocol. Here, $R_{\text{opt}}(\varepsilon_s, \varepsilon_{EA})$ is defined as (given fixed q, n)

$$g(p) = \begin{cases} 1 - h\left(\frac{1}{2} + \frac{1}{2}\sqrt{16\frac{p}{q}(\frac{p}{q} - 1) + 3}\right) & \frac{p}{q} \in [0, \frac{2+\sqrt{2}}{4}] \\ 1 & \frac{p}{q} \in [\frac{2+\sqrt{2}}{4}, 1] \end{cases} \quad (11)$$

$$f_{\min}(p, p_t) = \begin{cases} g(p) & p \leq p_t \\ \frac{d}{dp}g(p)|_{p_t} \cdot p + (g(p_t) - \frac{d}{dp}g(p)|_{p_t} \cdot p_t) & p > p_t \end{cases} \quad (12)$$

$$R(p, p_t, \varepsilon_s, \varepsilon_e) \quad (13)$$

$$= f_{\min}(p, p_t) - \frac{1}{\sqrt{n}} 2(\log 13 + \frac{d}{dp}g(p)|_{p_t}) \sqrt{1 - 2 \log(\varepsilon_s \cdot \varepsilon_e)}. \quad (14)$$

$$R_{\text{opt}}(\varepsilon_s, \varepsilon_e) = \max_{\frac{3}{4} < \frac{p_t}{q} < \frac{2+\sqrt{2}}{4}} R(\omega_{\text{exp}} \cdot q - \delta_{\text{est}}, p_t, \varepsilon_s, \varepsilon_e). \quad (15)$$

where ω_{exp} is the expected winning probability for an honest but noisy device, $\delta_{\text{est}} \in (0, 1)$ is the width of the statistical confidence interval for the Bell violation estimation test. Thus ω_{exp} can be chosen according to the experimental winning scores $\sum_i J_i$ and $\omega_{\text{exp}} = \sum_i J_i / n - 0.75$. A greater δ_{est} will lead to a higher randomness production. However, δ_{est} is bounded by the number of trials N and another error $\varepsilon_{Q\text{RNG}}^c$, which represents the completeness error of the entropy accumulation protocol,

$$\varepsilon_{Q\text{RNG}}^c \leq \exp(-2n\delta_{\text{est}}^2) \quad (16)$$

Considering the failure probability 2^{t_e} in the randomness extraction process, the soundness error for this protocol is

$$\varepsilon_{Q\text{RNG}}^s = \varepsilon_s + \varepsilon_{EA} + 2^{t_e}. \quad (17)$$

C. Optimal parameter q

Define the net randomness output to be the difference between the output and input randomness. In general, we can optimize the parameter q to find out the maximal net randomness output per round,

$$R_{\text{net}} = R_{\text{opt}}(\varepsilon_s, \varepsilon_{EA}) - h(q) - q \quad (18)$$

For example consider $\delta_{\text{est}} = 10^{-2}, \varepsilon_s = 10^{-6}, \varepsilon_{EA} = 10^{-6}, w_{\text{exp}} = \frac{2+\sqrt{2}}{4} - 0.75$, the optimal q which maximizes the R_{net} can be found by numerical search for a given n . Here we give a table for different n and the corresponding optimal q and R_{net} .

In our experiment, we set $q = 1$. As we do not use randomness to choose the measurement setting, the obtained randomness $nR_{\text{opt}}(\varepsilon_s, \varepsilon_{EA})$ is the net randomness output.

TABLE II. The relation between the net randomness rate, bias q , and number of experimental trials n .

n	q	R_{net}
10^7	-	0
10^8	0.0777	0.0256
10^9	0.0587	0.2175
10^{11}	0.0486	0.3279
10^{14}	0.0473	0.3417

D. Numerical result

As shown in Fig. 4, we consider the relation between the randomness output $R_{opt}(\varepsilon_s, \varepsilon_{EA})$ and the expected CHSH value ω_{exp} . Given the expected CHSH value ω_{exp} , we also show in Fig. 5 the minimal required number of trials to guarantee a nonzero randomness output.

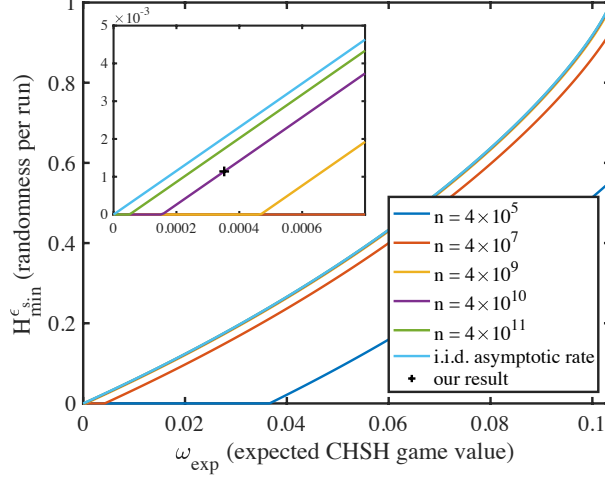


FIG. 4. Randomness generation with different expected violation. For the finite data rate curve, we set $\varepsilon_s = \varepsilon_{EA} = 1/\sqrt{n}$ and $\delta_{est} = \sqrt{10/n}$ for different number of experimental trials n .

Considering perfect state preparation and imperfect detection with efficiency η , the relation between the maximal expected CHSH value ω_{exp} and the efficiency is shown in Fig. 6. We also show the relation between the detection efficiency and the randomness output in Fig. 7.

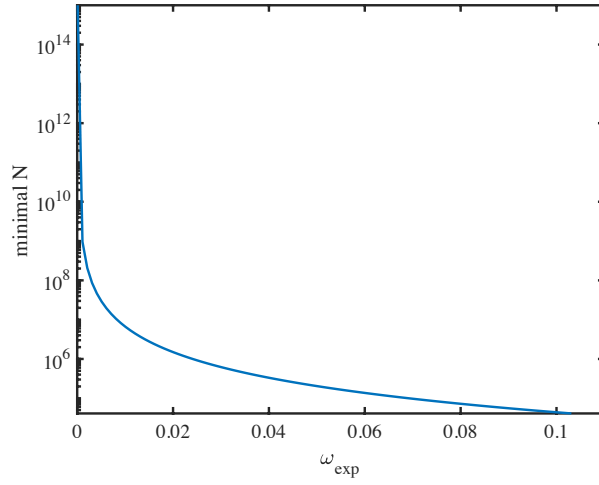


FIG. 5. Minimal number of experimental trials n that has a nonzero randomness generation rate for different expected violations. Here, we set $\varepsilon_s = \varepsilon_{\text{EA}} = 1/\sqrt{n}$ and $\delta_{\text{est}} = \sqrt{10/n}$ for different number of experimental trials n .

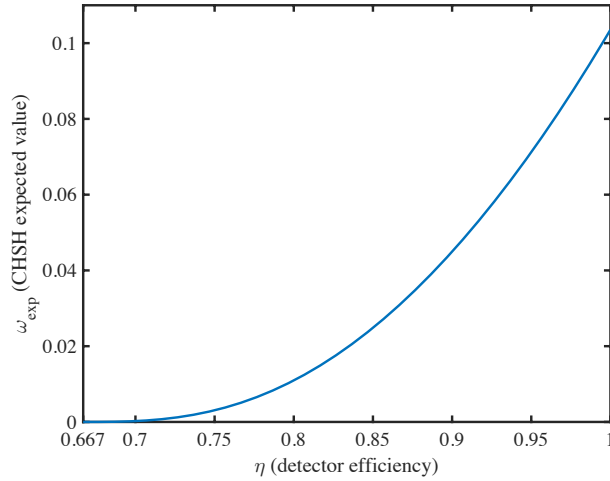


FIG. 6. Maximal expected CHSH value ω_{exp} with different detection efficiency, considering the perfect state preparation and imperfect detection with efficiency η .

II. ENTANGLEMENT CHARACTERIZATION

To characterize the entangled photon pairs, we set the mean photon number to $\mu = 0.004$ to decrease the multi-photon effect. We set the pump to be diagonal polarized $|+\rangle$, to generate the maximum entangled state $|\Psi^+\rangle = (|HV\rangle + |VH\rangle)/\sqrt{2}$. The visibility is measured under horizontal/vertical basis and diagonal/anti-diagonal basis, as $99.5 \pm 2.0\%$

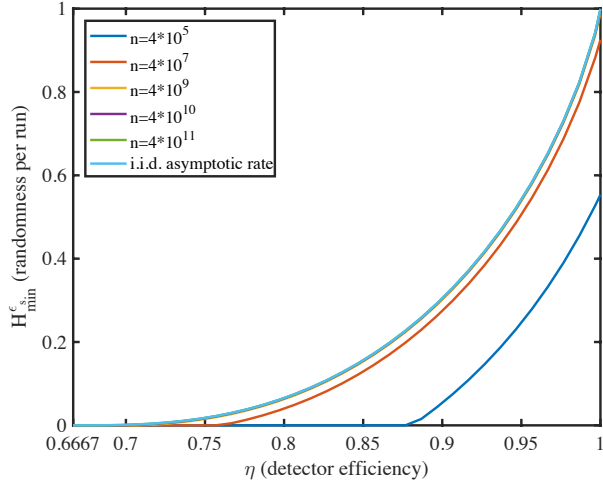


FIG. 7. Maximal randomness generation with different detection efficiency, considering the perfect state preparation and imperfect detection with efficiency η . For the finite data rate curve, we set $\epsilon_s = \epsilon_{\text{EA}} = 1/\sqrt{n}$ and $\delta_{\text{est}} = \sqrt{10/n}$ for different number of runs n .

and $97.8 \pm 1.5\%$. We attribute the imperfection to multi-photon components, imperfect optical elements, and imperfect spatial/spectral mode matching.

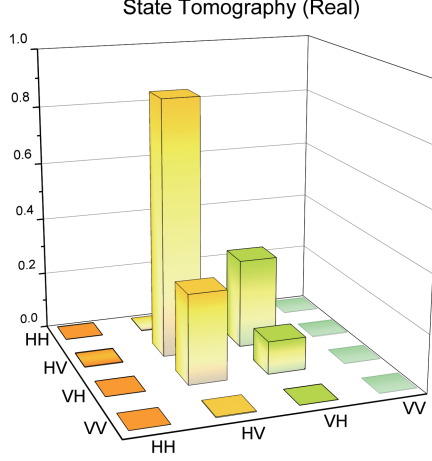
In testing the Bell inequality, we need to generate a non-maximally entangled state. Considering the system heralding efficiency and the visibility, we optimize the state and measurement basis based on 77% system efficiency, following Eberhard's original article [25]. The sub-optimal state is $\cos(20.5^\circ) |HV\rangle + \sin(20.5^\circ) |VH\rangle$ (with $r = 0.37$ for $(|HV\rangle + r|VH\rangle)/\sqrt{1+r^2}$). The measurement bases are $a_1 = -84.0^\circ$, $a_2 = -118.7^\circ$ for Alice, $b_1 = 6^\circ$, $b_2 = -28.7^\circ$ for Bob.

We perform state tomography on the non-maximally entangled state $\cos(20.5^\circ) |HV\rangle + \sin(20.5^\circ) |VH\rangle$. The result is shown in Fig. 8, the state fidelity is 99.3% compared to the ideal state.

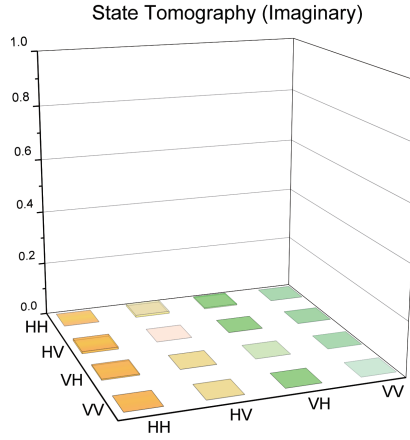
III. SYSTEM EFFICIENCY

The system efficiency is vital to close the detection loophole in Bell test. Normally, the system efficiency includes the following parts: the entanglement source, the transmission link, the detection. Here we consider each part individually.

The (system) heralding efficiency is defined as $\eta_s = C/N_i$ and $\eta_i = C/N_s$, where the



(a)



(b)

FIG. 8. (color online) Tomography of the produced state. The real and imaginary part are shown in (a) and (b), respectively.

coincidence events (C) and the signal (idler) events $N_s(N_i)$ can be measured during the experiment. If considering the optical efficiency η_{opt} and the detector efficiency $\eta_s^{det}(\eta_i^{det})$, the entangled pair collection efficiency is $\eta_s^{opt} = C/(N_i \cdot \eta_s^{det} \cdot \eta_{opt})$ and $\eta_i^{opt} = C/(N_s \cdot \eta_i^{det} \cdot \eta_{opt})$.

In a Sagnac based entanglement generation as we used in the experiment, a periodically poled potassium titanyl phosphate (PPKTP) crystal is used as the nonlinear material to generate photon pairs. The generated photon pairs will be collected into single mode fibers for further modulation and detection. Theory predictions [29] and experimental tests [24, 30] show it is possible to achieve a near unity heralding efficiency by selecting appropriate focal parameters. For our source, we adjust the pump light beam waist to be around $180 \mu m$,

and the collection beam waist to be around $85\ \mu\text{m}$ (see the setup section for detail). Theory predicts the collection efficiency for the photons is 98% if the PPKTP is 0.9 cm thick.

In detection, We uses high efficiency superconducting nanowire single-photon detectors (SNSPD) [31] to detect the received photons. The SNSPD is made of polycrystalline NbN, and can achieve its best performance (saturate) at around 1.8 K temperature. In our experiment, we cool the detector chips to less than 1K. In our test, the detectors are biased $0.2\ \mu\text{A}$ below their critical current for stable operation. The single photon detection efficiencies are 90.2% for Alice and 92.2% for Bob, with dark counts less than $100\ \text{s}^{-1}$.

We measure the (system) heralding efficiency to be $\eta_s = 78.6\% \pm 1.5\%$ for Alice and $\eta_i = 80.2\% \pm 1.5\%$ for Bob. The optical efficiency in the entanglement preparation is around 95.5%, the efficiency of the 130 meter fiber between the source and the detection is around 99%. We then estimate the entangled pair collection efficiency as $\eta_s^{opt} = 92.1\%$ for Alice and $\eta_i^{opt} = 92.0\%$ for Bob.

IV. DETAILED EXPERIMENTAL PARAMETERS

We focus the pump and collection mode to the center of the PPKTP crystal. In experiment, the pump light is spatial filtered by a 780HP single mode fiber. The light is the focused using a aspherical lens with $f=8\ \text{mm}$ to the PPKTP that is around 70 cm away. The pump waist is estimated to be $180\ \mu\text{m}$, and the beam quality M^2 is around 1.05.

For collection, we used SMF28e single mode fiber. An Aspherical lens with $f=11\ \text{mm}$ and a spherical lens with $f=175\ \text{mm}$ focus the beam to $85\ \mu\text{m}$ at the center of PPKTP. The spherical lens is placed in the middle, about 19 cm from the aspherical, and about 45 cm from the PPKTP.

We measure the efficiencies of the optical elements individually, as shown in Tab. III.

The dimension of PPKTP we used is $1\ \text{mm} \times 2\ \text{mm} \times 10\ \text{mm}$, with a poling period of $46.5\ \mu\text{m}$. In our experiment, the pump power is about 3.5 mw, to create 15000 pairs entangled photons per second.

TABLE III. The efficiencies of optical elements

Optical element	Efficiency
Aspherical lens	$99.27\% \pm 0.03\%$
Spherical lens	$99.6\% \pm 1.0\%$
Half wave plate (780nm/1560nm)	$99.93\% \pm 0.02\%$
Half wave plate (1560nm)	$99.92\% \pm 0.04\%$
Quater wave plate (1560nm)	$99.99\% \pm 0.08\%$
Polarization beam splitter (780nm/1560nm)	$99.6\% \pm 0.1\%$
Polarization beam splitter (1560nm)	$99.6\% \pm 0.2\%$
Silicon plate	$99.7\% \pm 0.2\%$
Dichromatic mirror	$99.46\% \pm 0.03\%$
PPKTP	$99.6\% \pm 0.2\%$

V. THE BELL INEQUALITY VIOLATION WITH DIFFERENT MEAN PHOTON NUMBER

In the experiment, we set the mean photon number to be around 0.15 per pulse. As shown in Tab. V, the violation is $J_n = 3.52 \times 10^{-4}$ for 4×10^{10} trials. While previous experiments used small mean photon number to reduce the multi-photon effect, we find an optimized mean photon number by modeling the Bell test with multi-photons. When the mean photon number is small, the quantum states in most of the experimental trials are vacuum. Increasing mean photon number will increase the proportion of non vacuum states and increase the Bell violation. The violation will decrease when the multi-photon effect becomes significant. We find the optimal violation by numerical simulation, the results are given in Tab. III-VIII.

VI. SIMULATION

In our simulation, we consider the i.i.d. case. We will only focus on the probability distribution. Furthermore, we consider that the experiment observes the no-signaling theorem. In this case, we can equivalently consider the CH inequality. The CH inequality is a bipartite Bell inequality with measurement settings $x \in \{0, 1\}$ and $y \in \{0, 1\}$, and out-

TABLE IV. The CHSH violation with different mean photon numbers.

Mean photon number	CHSH violation
0.005	1.58×10^{-5}
0.01	6.29×10^{-5}
0.02	9.72×10^{-5}
0.05	1.99×10^{-4}
0.1	2.50×10^{-4}
0.15	3.52×10^{-4}
0.2	2.48×10^{-4}

TABLE V. Number of correlated events for equal number of trials (10^{10}) per measurement base settings: A_1B_1 , A_1B_2 , A_2B_1 and A_2B_2 . $a = 0$ or 1 indicates that Alice detects a photon or not, the same b for Bob. Mean photon number $\mu = 0.15$, violation $J_n = 3.52 \times 10^{-4}$.

Basis settings	$ab = 00$	$ab = 10$	$ab = 01$	$ab = 11$
A_1B_1	9780816728	49862593	57002217	112318462
A_1B_2	9574958251	41366122	263425568	120250059
A_2B_1	9577555854	253683380	46874032	121886734
A_2B_2	9255451323	361101111	365181363	18266203

puts $a, b \in \{0, 1, u\}$, corresponding to 0, 1, and undetected events, respectively. The CH

TABLE VI. Number of correlated events for equal number of trials (5×10^7) per measurement base settings. Mean photon number $\mu = 0.2$, violation $J_n = 2.48 \times 10^{-4}$.

Basis settings	$ab = 00$	$ab = 10$	$ab = 01$	$ab = 11$
A_1B_1	48453853	355764	397898	792485
A_1B_2	46955670	294787	1884426	865117
A_2B_1	46947701	1847449	331927	872923
A_2B_2	44662839	2563681	2598180	175300

TABLE VII. Number of correlated events for equal number of trials (5×10^7) per measurement base settings. Mean photon number $\mu = 0.1$, violation $J_n = 2.50 \times 10^{-4}$.

Basis settings	$ab = 00$	$ab = 10$	$ab = 01$	$ab = 11$
$A_1 B_1$	49312617	155809	185673	345901
$A_1 B_2$	48633646	127616	867571	371167
$A_2 B_1$	48652215	825815	149637	372333
$A_2 B_2$	47597903	1165406	1196733	39958

TABLE VIII. Number of correlated events for equal number of trials (5×10^7) per measurement base settings. Mean photon number $\mu = 0.05$, violation $J_n = 1.99 \times 10^{-4}$.

Basis settings	$ab = 00$	$ab = 10$	$ab = 01$	$ab = 11$
$A_1 B_1$	49657069	78257	92401	172273
$A_1 B_2$	49318372	65894	429597	186137
$A_2 B_1$	49321033	413099	78382	187486
$A_2 B_2$	48789537	591262	606143	13058

inequality is a linear combination of the probability distribution $p(a, b|x, y)$ and given by

$$\begin{aligned}
J_{CH} = & -p_{00}(0, 0) - p_{00}(0, 1) - p_{00}(1, 0) \\
& + p_{00}(1, 1) + p_0^A(0) + p_0^B(0) \geq 0.
\end{aligned} \tag{19}$$

Here, we take a more convenient notation of $p(a, b|x, y)$ as $p_{ab}(x, y)$, and $p_0^A(0)$ ($p_0^B(0)$) refers to the probability of obtaining 0 when Alice's (Bob's) input is 0 (0). Suppose the Bell value

TABLE IX. Number of correlated events for equal number of trials (5×10^7) per measurement base settings. Mean photon number $\mu = 0.02$, violation $J_n = 9.72 \times 10^{-5}$.

Basis settings	$ab = 00$	$ab = 10$	$ab = 01$	$ab = 11$
$A_1 B_1$	49848404	36312	39931	75353
$A_1 B_2$	49692655	31079	192707	83559
$A_2 B_1$	49686075	192384	35158	86383
$A_2 B_2$	49448963	272187	274815	4035

TABLE X. Number of correlated events for equal number of trials (1×10^8) per measurement base settings. Mean photon number $\mu = 0.01$, violation $J_n = 6.29 \times 10^{-5}$.

Basis settings	$ab = 00$	$ab = 10$	$ab = 01$	$ab = 11$
A_1B_1	99837479	38578	42882	81061
A_1B_2	99671930	33487	205544	89039
A_2B_1	99651185	213872	40318	94625
A_2B_2	99396430	298159	301665	3746

TABLE XI. Number of correlated events for equal number of trials (3.58×10^8) per measurement base settings. Mean photon number $\mu = 0.005$, violation $J_n = 3.30 \times 10^{-5}$.

Basis settings	$ab = 00$	$ab = 10$	$ab = 01$	$ab = 11$
A_1B_1	357726090	65895	74068	133947
A_1B_2	357459604	57387	338791	144218
A_2B_1	357495160	309855	58769	136216
A_2B_2	357043095	476212	475809	4884

of the CHSH inequality is J_{CHSH} , the relation is

$$J_{CHSH} = -J_{CH}/2. \quad (20)$$

The prepared quantum state is in the form of

$$|\psi\rangle = \frac{1}{\sqrt{1+r^2}}(|HV\rangle + r|VH\rangle). \quad (21)$$

The measurement of Alice and Bob are projective measurement in the following basis

$$\{\cos\alpha|H\rangle + \sin\alpha|V\rangle, -\sin\alpha|H\rangle + \cos\alpha|V\rangle\}. \quad (22)$$

With given detection efficiency, the optimal state and measurement can be numerically found.

Apart from the detection efficiency, other experimental imperfections such as imperfect photon source, background noise, misalignment error should be taken into account in order to simulate the experiment.

A. Imperfect input state

To achieve an optimal violation of the CH inequality, we prepare quantum state in the form of Eq. (21). In practice, the experimentally prepared input state may be imperfect, deviating from the desired one. One way is to model the imperfectly prepared state by

$$\rho = \frac{1}{1+r^2} \begin{pmatrix} 0 & 0 & 0 & 0 \\ 0 & 1 & Vr & 0 \\ 0 & Vr & r^2 & 0 \\ 0 & 0 & 0 & 0 \end{pmatrix}, \quad (23)$$

where V can be interpreted as the visibility along a certain measurement direction. Thus a smaller V represents a larger imperfection. In experiment, we can also perform a state tomography to directly get an estimation of the prepared state.

B. SPDC source

The photon pair distribution of an SPDC source follows a Poisson distribution,

$$P(n) = \frac{\mu^n}{n!} e^{-\mu}. \quad (24)$$

or a thermal distribution,

$$P(n) = \frac{\mu^n}{(1+\mu)^{n+1}} e^{-\mu}, \quad (25)$$

where μ is the mean photon number. In this case, the source may emit vacuum with probability $P(0)$, one pair with probability $P(1)$, two pairs with probability $P(2)$, and so on. When considering no background, the vacuum part contributes 0 to the Bell value and the rest part contributes positive Bell value.

In the following, we will evaluate the Bell value with multiple photon pairs. As the probability of multiple photon pairs is very small, we only calculate the averaged Bell value J_2 with two photon pairs as input. We consider threshold detector in our simulation.

In general, there are two detectors for each measurement. For single photon pairs, there are nine exclusive events as shown in Table XII. For two photon pairs, there are $9 \times 9 = 81$ exclusive events. However, when threshold detectors are used, there are only 4 different distinguishable events for Alice (Bob), including, 0, 1, u, and double click (detecting 0 and 1 at the same time). As the output of the original CH inequality has only three distinct

TABLE XII. Possible events for single photon pair.

parties	1	2	3	4	5	6	7	8	9
Alice	0	0	0	1	1	1	u	u	u
Bob	0	1	u	0	1	u	0	1	u

outputs for each party, we thus need to assign an output (0, 1, or u) for the events of double clicks.

Generally, when a double click happens, we randomly assign the output value to be 0, 1, or u, with probability q_0 , q_1 , and q_u , respectively. For example, when the 00 and 01 events happens for the two pairs, Alice will detect oo and thus also output o, while Bob will detect 01 and output 0 or 1 with additional probability q_0 or q_1 , respectively. When $q_0 = 1$ it corresponds to the case that double click events are all assigned to output of 0 which corresponds to the case that only one detector is used for each party.

After the random assignment, the output contains nine exclusive events. Note that, by saying double click, we actually mean the events of detecting 0 and 1 at the same time. For the other cases, for instance, when detecting 0 and u or 0 and 0 at the same time, we simply assign the output to be 0 deterministically. This is because that we cannot distinguish between the events of 0u, u0, and 00 for each party in experiment.

It is worth mentioning that the random assignment must be performed instantly after a measurement outcome is observed, such that Alice and Bob cannot communicate. That is, the events of random assignments of Alice and Bob must be space-likely separated. In experiment, such requirement can be satisfied by considering that random assignment is delay-processed in data postprocessing. In this case, the random assignment strategies of Alice and Bob should be fixed before experiment. This requirement can be fulfilled by introducing a trusted referee to perform the data postprocessing. He will honestly perform the random assignment of the data from Alice and Bob with a predetermined strategy.

Suppose the underlying probability distribution of the nine events with single photon pair conditioned on specific input setting x and y are denoted by $p_i(x, y)$ for experimental trial i , we can calculate the probability $p_1^{n=2}(x, y)$ of obtaining 00 with two pairs of photons after the assignment by

$$p_1^{n=2}(x, y) = \sum_{i,j} \beta_{ij} p_i(x, y) p_j(x, y), \quad (26)$$

where the coefficients β_{ij} are given by

$$\beta_{ij} = \begin{pmatrix} 1 & q_0^a & 1 & q_0^b & q_0^a q_0^b & q_0^a & 1 & q_0^b & 1 \\ q_0^a & 0 & 0 & q_0^a q_0^b & 0 & 0 & q_0^b & 0 & 0 \\ 1 & 0 & 0 & q_0^a & 0 & 0 & 1 & 0 & 0 \\ q_0^b & q_0^a q_0^b & q_0^a & 0 & 0 & 0 & 0 & 0 & 0 \\ q_0^a q_0^b & 0 & 0 & 0 & 0 & 0 & 0 & 0 & 0 \\ q_0^a & 0 & 0 & 0 & 0 & 0 & 0 & 0 & 0 \\ 1 & q_0^b & 1 & 0 & 0 & 0 & 0 & 0 & 0 \\ q_0^b & 0 & 0 & 0 & 0 & 0 & 0 & 0 & 0 \\ 1 & 0 & 0 & 0 & 0 & 0 & 0 & 0 & 0 \end{pmatrix}, \quad (27)$$

where q_0^a and q_0^b refer to the random assignment probability of Alice and Bob, respectively.

For single party detections, there are three types of events: 0, 1, and u. When there are two pairs, we can similarly assign double click events. For instance, for single detection probability $p_1^A(x)$, where 1 also stands for event o, we have the corresponded one for two pairs,

$$p_1^{A,n=2}(x) = \sum_{i,j} \beta'_{ij} p_i^A(x) p_j^A(x), \quad (28)$$

with coefficient defined by

$$\beta'_{ij} = \begin{pmatrix} 1 & q_0^a & 1 \\ q_0^a & 0 & 0 \\ 1 & 0 & 0 \end{pmatrix} \quad (29)$$

Thus, we can calculate the normalized contribution from two pairs, denoted by $\bar{J}_{n=2}$ according to Eq. (26) and Eq. (28). Then a weighted Bell value is given by

$$J \approx P(1)J_{n=1} + P(2)J_{n=2}. \quad (30)$$

C. Misalignment error

Due to imperfection in detection, there may also be misalignment error which outputs value opposite to the real one. Suppose the rate of misalignment error is p_M , then each party will output 0 (1) when its actual value is 1 (0) with probability p_M . Denote the events by the index in Table. XII, then the coincidence probability after misalignment is

$$p_i^M(x, y) = \sum_i \gamma_{ij} p_j(x, y), \forall i \quad (31)$$

where the coefficients γ_{ij} is given by

$$\gamma_{ij} = \begin{pmatrix} (1-p_M)^2 & (1-p_M)p_M & 0 & (1-p_M)p_M & p_M^2 & 0 & 0 & 0 & 0 \\ (1-p_M)p_M & (1-p_M)^2 & 0 & p_M^2 & (1-p_M)p_M & 0 & 0 & 0 & 0 \\ 0 & 0 & (1-p_M) & 0 & 0 & p_M & 0 & 0 & 0 \\ (1-p_M)p_M & p_M^2 & 0 & (1-p_M)^2 & (1-p_M)p_M & 0 & 0 & 0 & 0 \\ p_M^2 & (1-p_M)p_M & 0 & (1-p_M)p_M & (1-p_M)^2 & 0 & 0 & 0 & 0 \\ 0 & 0 & p_M & 0 & 0 & (1-p_M) & 0 & 0 & 0 \\ 0 & 0 & 0 & 0 & 0 & 0 & (1-p_M) & p_M & 0 \\ 0 & 0 & 0 & 0 & 0 & 0 & p_M & (1-p_M) & 0 \\ 0 & 0 & 0 & 0 & 0 & 0 & 0 & 0 & 1 \end{pmatrix},$$

For single detections, such as $p_0^A(x)$, we similarly have

$$p_0^{A,M}(x) = (1-p_M)p_0^A(x) + p_M p_1^A(x). \quad (32)$$

D. Dark count

In this part, we consider how background affects the experiment. Suppose the background is described by p_B , which denotes the probability of detecting a dark count for each detector. For instance, when the number of emitted pulses and dark counts are n and B for each detector, then $p_B = B/n$.

Due to the existence of dark counts, the Bell value will be affected when the input is vacuum. For coincidence detection $p_{00}(x, y)$, the probability contributed from dark counts is $p_{00}^{B,n=0}(x, y) = p_B^2$; for single detection $p_0^A(x)$, the probability contributed from dark counts is $p_0^{B,n=0}(x) = p_B$.

For the inputs with nonzero photon pairs, the situation becomes more complicated. For instance, when the source emit one photon pair, the probability contributed from dark counts

of coincidence detection $p_{00}(x, y)$ is

$$p_{00}^{B,n=1}(x, y) = p_{00}(x, y)\eta_a(1 - \eta_b)p_B + p_{00}(x, y)(1 - \eta_a)\eta_b p_B \\ + p_{00}(x, y)(1 - \eta_a)(1 - \eta_b)p_B^2 + (1 - p_{00}(x, y))p_B^2, \quad (33)$$

where the four terms correspond to four cases of the detection of the photon pair: Bob detects vacuum due to loss, Alice detect vacuum due to loss, Alice and Bob both detect vacuum due to loss, Alice and Bob detect other events. Here, we only consider that Alice and Bob each use one detector. The result is only slightly different when they each use two detectors.

Denote the normalized contribution from dark count by J_B , then the total Bell value J is given by

$$J \approx J_B + P(1)J_{n=1} + P(2)J_{n=2}. \quad (34)$$

In our simulation, we first generate the probability distribution by using the quantum state from tomography. Then, we consider misalignment error and multi-photon states. Finally, we take into account the contribution from background noise.

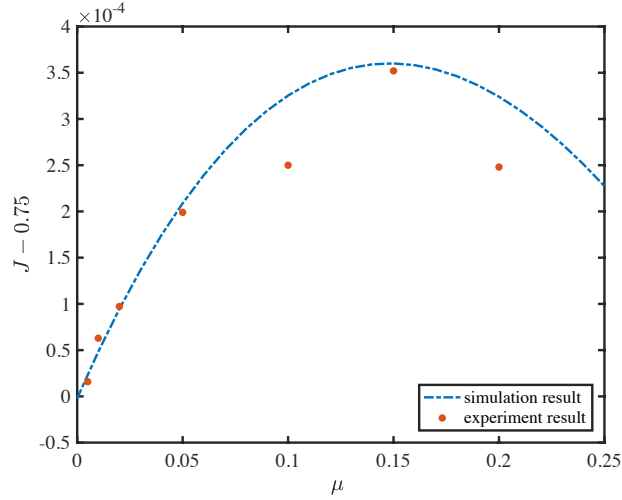


FIG. 9. Simulation result. The relation between Bell inequality violation and mean photon number.

In our simulation, we set $p_B = 2 \times 10^{-6}$ and $p_M = 0.002$.

VII. RANDOMNESS EXTRACTION

Toeplitz extractor is used for randomness extraction from raw data [32, 33]. In total, we have 4×10^{10} experimental trials. 2 bits are used to record the detection results in each trial.

For instance, $a = 0, b = 1$ represent that Alice does not detect a photon while Bob detects one photon, which is noted as $ab = 01$ in the text. As a result, 8×10^{10} bits of raw data are collected. Multiplying a Toeplitz matrix with dimensions $m \times n = (4.56 \times 10^7) \times (8 \times 10^{10})$ to the raw data vector with a dimension $n = 8 \times 10^{10}$ yields a vector with a dimension $m = 4.56 \times 10^7$.

A $m \times n$ Toeplitz matrix takes the form:

$$T_{m \times n} = \begin{pmatrix} a_0 & a_{-1} & \cdots & a_{-(n-2)} & a_{-(n-1)} \\ a_1 & a_0 & \ddots & & a_{-(n-1)+1} \\ a_2 & a_1 & \ddots & \ddots & \vdots \\ \vdots & \vdots & & \ddots & a_{-(n-1)+(m-2)} \\ a_{m-1} & a_{m-2} & \cdots & a_{-n+(m-1)} & a_{-(n-1)+(m-1)} \end{pmatrix} \quad (35)$$

with raw data vector:

$$V_n = \begin{pmatrix} v_0 \\ v_1 \\ v_2 \\ \vdots \\ v_{n-1} \end{pmatrix} \quad (36)$$

The result is:

$$R_m = \begin{pmatrix} r_0 \\ r_1 \\ r_2 \\ \vdots \\ r_{m-1} \end{pmatrix} \quad (37)$$

The result random number is obtained by a multiplication between a Toeplitz matrix and a vector:

$$R_m = T_{m \times n} \times V_n \quad (38)$$

An fast Fourier transform (FFT) can be applied to speed up the multiplication:

$$T_{m \times n} \times V_n = IFFT(FFT(T_{m+n-1}) \cdot FFT(V_m)) \quad (39)$$

Here FFT is the fast Fourier transform on the vector, T_{m+n-1} is the elements $(a_{-(n-1)}, \dots, a_{-1}, a_0, a_1, \dots, a_m)$ in the Toeplitz matrix. IFFT is the inverse fast Fourier transform of the product of the

vectors. In calculation, the vector dimension should be expand to $m+n-1$ by adding zeros at the end.

In our experiment, we divide the matrix into $k = n/l$ blocks each with dimension $m \times l$:

$$T_{m \times n} = \begin{pmatrix} T_{m \times l}^0 & T_{m \times l}^1 & \cdots & T_{m \times l}^{k-1} \end{pmatrix} \quad (40)$$

and the block $T_{m \times l}^i$ is:

$$T_{m \times l}^i = \begin{pmatrix} a_{-i \cdot l} & a_{-(i \cdot l + 1)} & \cdots & a_{-(i \cdot l + l - 1)} \\ a_{-i \cdot l + 1} & a_{-i \cdot l} & \ddots & a_{-(i \cdot l + l - 1) + 1} \\ \vdots & \vdots & & \vdots \\ a_{-i \cdot l + m - 1} & a_{-i \cdot l + m - 2} & \cdots & a_{-(i \cdot l + l - 1) + m - 1} \end{pmatrix} \quad (41)$$

Similarly, the vector is divided into k blocks:

$$V_n = \begin{pmatrix} V_l^0 \\ V_l^1 \\ \vdots \\ V_l^{k-1} \end{pmatrix} \quad (42)$$

with each block:

$$V_l^i = \begin{pmatrix} v_{i \cdot l} \\ v_{i \cdot l + 1} \\ \vdots \\ v_{i \cdot l + l - 1} \end{pmatrix} \quad (43)$$

For each block, FFT speed up can be applied, and a series of blocks of result is obtained:

$$R'_m = \begin{pmatrix} R_l^0 & R_l^1 & \cdots & R_l^{k-1} \end{pmatrix} \quad (44)$$

where $R_l^i = T_{m \times l}^i \cdot V_l^i$, with each block:

$$R_l^i = \begin{pmatrix} r_0^i \\ r_1^i \\ \vdots \\ r_{m-1}^i \end{pmatrix} \quad (45)$$

Finally, each row of the result block is added to give the result:

$$R_m = \begin{pmatrix} \Sigma_i r_0^i \\ \Sigma_i r_1^i \\ \vdots \\ \Sigma_i r_{m-1}^i \end{pmatrix} \quad (46)$$

The blocked algorithm is slower than the full FFT algorithm, but it saves memory. We perform the extraction calculation on a personal computer with 16 Gbytes memory by dividing the original data into 800 blocks, which takes 17 hrs including data loading and computation.

VIII. STATISTICAL ANALYSIS

We obtain 4.56×10^7 random bits. We use 45 M bits data with section length set to 450 K bits for NIST statistical test [34]. As shown in Tab. XIII, the random bits successfully pass the NIST tests.

-
- [1] X. Ma, X. Yuan, Z. Cao, B. Qi, and Z. Zhang, npj Quantum Information **2**, 16021 (2016).
 - [2] M. Herrero-Collantes and J. C. Garcia-Escartin, Rev. Mod. Phys. **89**, 015004 (2017).
 - [3] R. Colbeck, *Quantum And Relativistic Protocols For Secure Multi-Party Computation*, Ph.D. thesis, PhD Thesis, 2009 (2009).
 - [4] R. Colbeck and R. Renner, Nature Physics **8**, 450 (2012), arXiv:1105.3195 [quant-ph].
 - [5] S. Fehr, R. Gelles, and C. Schaffner, Phys. Rev. A **87**, 012335 (2013).
 - [6] S. Pironio and S. Massar, Phys. Rev. A **87**, 012336 (2013).
 - [7] U. Vazirani and T. Vidick, Phys. Rev. Lett. **113**, 140501 (2014).
 - [8] C. A. Miller and Y. Shi, in *Proceedings of the 46th Annual ACM Symposium on Theory of Computing*, STOC '14 (ACM, New York, NY, USA, 2014) pp. 417–426.
 - [9] K.-M. Chung, Y. Shi, and X. Wu, arXiv preprint arXiv:1402.4797 (2014).
 - [10] M. Coudron and H. Yuen, in *Proceedings of the 46th Annual ACM Symposium on Theory of Computing* (ACM, 2014) pp. 427–436.
 - [11] C. A. Miller and Y. Shi, arXiv preprint arXiv:1411.6608 (2014).

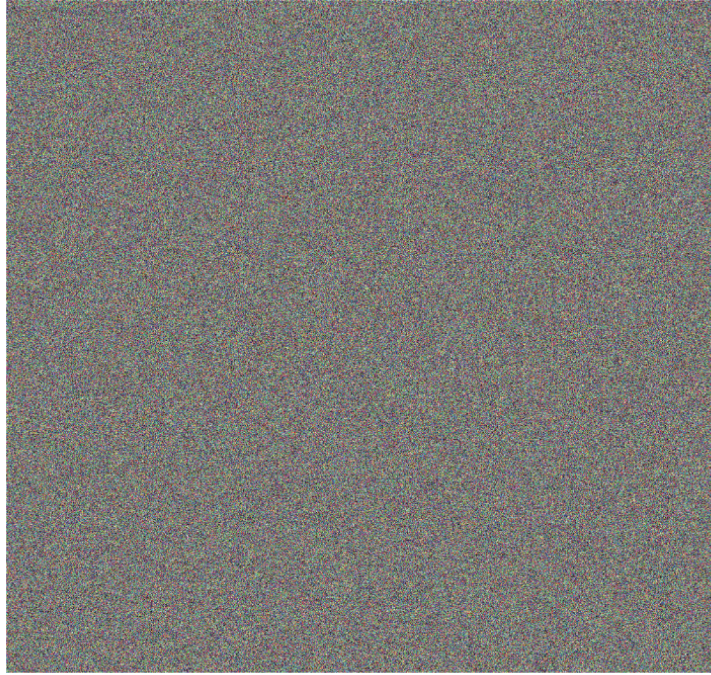
TABLE XIII. Results of the NIST test suite using 45 Mbit of data (100 sequences of 450 Kbit) with the generated random numbers.

Statistical tests	P value	Proportion	Result
Frequency	0.63712	1.000	Success
BlockFrequency	0.22482	0.980	Success
CumulativeSums	0.37040	1.000	Success
Runs	0.33454	1.000	Success
LongestRun	0.61631	1.000	Success
Rank	0.30413	0.990	Success
FFT	0.77919	1.000	Success
NonOverlappingTemplate	0.71975	0.991	Success
OverlappingTemplate	0.09320	1.000	Success
Universal	0.36692	0.970	Success
ApproximateEntropy	0.51412	1.000	Success
RandomExcursions	0.38200	0.995	Success
RandomExcursionsVariant	0.41480	0.995	Success
Serial	0.42510	0.995	Success
LinearComplexity	0.91141	0.990	Success

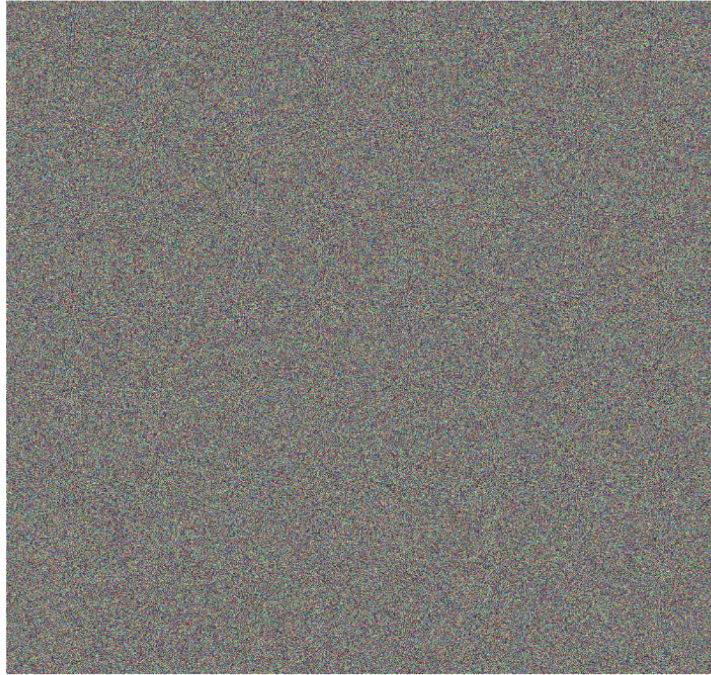
- [12] F. Dupuis, O. Fawzi, and R. Renner, arXiv preprint arXiv:1607.01796 (2016).
- [13] R. Arnon-Friedman, R. Renner, and T. Vidick, arXiv preprint arXiv:1607.01797 (2016).
- [14] S. Pironio, A. Acín, S. Massar, A. B. de La Giroday, D. N. Matsukevich, P. Maunz, S. Olmschenk, D. Hayes, L. Luo, T. A. Manning, *et al.*, Nature **464**, 1021 (2010).
- [15] B. G. Christensen, K. T. McCusker, J. B. Altepeter, B. Calkins, T. Gerrits, A. E. Lita, A. Miller, L. K. Shalm, Y. Zhang, S. W. Nam, N. Brunner, C. C. W. Lim, N. Gisin, and P. G. Kwiat, Phys. Rev. Lett. **111**, 130406 (2013).
- [16] B. Hensen, H. Bernien, A. Dréau, A. Reiserer, N. Kalb, M. Blok, J. Ruitenberg, R. Vermeulen, R. Schouten, C. Abellán, *et al.*, Nature **526**, 682 (2015).
- [17] L. K. Shalm, E. Meyer-Scott, B. G. Christensen, P. Bierhorst, M. A. Wayne, M. J. Stevens, T. Gerrits, S. Glancy, D. R. Hamel, M. S. Allman, K. J. Coakley, S. D. Dyer, C. Hodge, A. E. Lita, V. B. Verma, C. Lambrocco, E. Tortorici, A. L. Migdall, Y. Zhang, D. R. Kumor, W. H.

- Farr, F. Marsili, M. D. Shaw, J. A. Stern, C. Abellán, W. Amaya, V. Pruneri, T. Jennewein, M. W. Mitchell, P. G. Kwiat, J. C. Bienfang, R. P. Mirin, E. Knill, and S. W. Nam, Phys. Rev. Lett. **115**, 250402 (2015).
- [18] M. Giustina, M. A. M. Versteegh, S. Wengerowsky, J. Handsteiner, A. Hochrainer, K. Phelan, F. Steinlechner, J. Kofler, J.-A. Larsson, C. Abellán, W. Amaya, V. Pruneri, M. W. Mitchell, J. Beyer, T. Gerrits, A. E. Lita, L. K. Shalm, S. W. Nam, T. Scheidl, R. Ursin, B. Wittmann, and A. Zeilinger, Phys. Rev. Lett. **115**, 250401 (2015).
- [19] W. Rosenfeld, D. Burchardt, R. Garthoff, K. Redeker, N. Ortegel, M. Rau, and H. Weinfurter, arXiv preprint arXiv:1611.04604 (2016).
- [20] J. Gallicchio, A. S. Friedman, and D. I. Kaiser, Phys. Rev. Lett. **112**, 110405 (2014).
- [21] J. Handsteiner, A. S. Friedman, D. Rauch, J. Gallicchio, B. Liu, H. Hosp, J. Kofler, D. Bricher, M. Fink, C. Leung, A. Mark, H. T. Nguyen, I. Sanders, F. Steinlechner, R. Ursin, S. Wengerowsky, A. H. Guth, D. I. Kaiser, T. Scheidl, and A. Zeilinger, Phys. Rev. Lett. **118**, 060401 (2017).
- [22] C. Wu, B. Bai, Y. Liu, X. Zhang, M. Yang, Y. Cao, J. Wang, S. Zhang, H. Zhou, X. Shi, X. Ma, J.-G. Ren, J. Zhang, C.-Z. Peng, J. Fan, Q. Zhang, and J.-W. Pan, Phys. Rev. Lett. **118**, 140402 (2017).
- [23] J. F. Clauser, M. A. Horne, A. Shimony, and R. A. Holt, Phys. Rev. Lett. **23**, 880 (1969).
- [24] M. Pereira, F. Becerra, B. Glebov, J. Fan, S. Nam, and A. Migdall, Opt Lett **38**, 1609 (2013).
- [25] P. H. Eberhard, Phys. Rev. A **47**, R747 (1993).
- [26] P. Bierhorst, E. Knill, S. Glancy, A. Mink, S. Jordan, A. Rommal, Y.-K. Liu, B. Christensen, S. W. Nam, and L. K. Shalm, arXiv preprint arXiv:1702.05178 (2017).
- [27] M. Coudron, T. Vidick, and H. Yuen, “Robust randomness amplifiers: Upper and lower bounds,” in *Approximation, Randomization, and Combinatorial Optimization. Algorithms and Techniques: 16th International Workshop, APPROX 2013, and 17th International Workshop, RANDOM 2013, Berkeley, CA, USA, August 21-23, 2013. Proceedings*, edited by P. Raghavendra, S. Raskhodnikova, K. Jansen, and J. D. P. Rolim (Springer Berlin Heidelberg, Berlin, Heidelberg, 2013) pp. 468–483.
- [28] S. Pironio, A. Acin, N. Brunner, N. Gisin, S. Massar, and V. Scarani, New Journal of Physics **11**, 045021 (2009).
- [29] R. Bennink, Phys Rev A **81**, 053805 (2010).

- [30] P. Dixon, D. Rosenberg, V. Stelmakh, M. Grein, R. Bennink, E. Dauler, A. Kerman, R. Molnar, and F. Wong, Phys Rev A **90** (2014), 10.1103/PhysRevA.90.043804.
- [31] W. Zhang, L. You, H. Li, J. Huang, C. Lv, L. Zhang, X. Liu, J. Wu, Z. Wang, and X. Xie, arXiv preprint arXiv:1609.00429 (2016).
- [32] R. Impagliazzo, L. A. Levin, and M. Luby, in *Proceedings of the twenty-first annual ACM symposium on Theory of computing*, STOC '89 (ACM, New York, NY, USA, 1989) pp. 12–24.
- [33] D. Frauchiger, R. Renner, and M. Troyer, arXiv preprint arXiv:1311.4547 (2013).
- [34] “Nist statistical tests suite,” http://csrc.nist.gov/groups/ST/toolkit/rng/stats_tests.html.



(a)



(b)

FIG. 10. Then final random numbers are divided into two parts (a) and (b), each figure contains 1000×950 pixels. For each pixel, 3 bytes random data are used to control the RGB color. All the random numbers generated in the experiment are used to draw the two figures.